Hydrodynamic Coefficients of Heave Plates, With Application to Wave Energy Conversion

Adam Brown, Jim Thomson, and Curtis Rusch

***Abstract*—Wave energy converters (WECs) often employ submerged heave plates to provide reaction forces at depths below the level of wave motion. Here, two sets of heave plate experiments are described, at varying scale. First, the Oscillator uses a linear actuator to force laboratory scale (30.5-cm diameter) heave plates in sinusoidal motion. Second, the miniWEC buoy uses vessel wakes to force field scale (1.5-m diameter) heave plates in open water with realistic energy conversion (damping). The motion and forces are analyzed using the Morison equation, in which the hydrodynamic coefficients of added mass C_M and drag C_D are determined for each set of Oscillator and miniWEC experiments. Results show strong intracycle variations in these coefficients, yet constant hydrodynamic coefficients provide a reasonable reconstruction of the time series data. The two test scales are examined relative to the Keulegan–Carpenter number (KC), Reynold's number (Re), and Beta number (β). The effects of asymmetric shape on hydrodynamic performance are found to be small.**

***Index Terms*—Added mass, coefficients, converter, drag, energy, heave, hydrodynamic, plate, power, reaction, wave, wave energy converter (WEC).**

I. Introduction

WAVE energy converters (WECs) harvest energy from the waves moving across the surface of the ocean. Waves excite motion in one or more bodies of the WEC, and power is produced as the WEC's power takeoff resists the relative motion of the bodies. The reaction forces associated with this resistance are transferred to the inertia of the system, thus power production is dependent on system mass. The cost of a WEC also depends, in part, on its material mass. Heave plates may be an effective means of reducing the mass and cost of a WEC while maintaining the maximum power output.

Heave plates, for wave energy conversion, are structures attached to or suspended from a WEC at a depth where the water is relatively still. Heave plates transfer the reaction loads developed by the WEC to the surrounding water. Heave plates have become a critical component of many WEC designs, and interest in their hydrodynamic behavior has increased [1]–[5]. Heave plates are also commonly used to stabilize offshore platforms, and a body of literature has developed focused on the use of heave plates for motion reduction [6], [7].

Hydrodynamic forces in oscillatory flow are often modeled using the Morison equation, which was originally developed to describe the force on a vertical pile due to oscillations of the surrounding water [8]. The Morison equation can also be used to model the hydrodynamic forces on a heave plate [6], [9]. In this case, the water is typically assumed stationary, therefore the relative motion is solely due to the oscillation of the heave plate vertically through the water column (this assumption is discussed in Section III).

The Morison equation provides an estimate of the force acting on the heave plate due to the surrounding water F_{Mor}. F_{Mor} comprises drag and inertial components as

$$F_{\mathrm{Mor}} = F_D + F_M = C_D\left(\tfrac{1}{2}\rho A u\,|u|\right) + C_M M\dot{u}. \quad (1)$$

The drag force F_D is the component of the Morison force related to the heave plate velocity u. Drag can be classified into two types, viscous drag, which increases linearly with velocity, and form drag, which increases quadratically with velocity. For heave plates oriented normal to the flow, viscous drag is small compared to form drag, and will not be considered. Assuming the water surrounding the heave plate is still, the drag force is assumed to be proportional to u^2, and to the projected area of the heave plate normal to the flow (A). The constant of proportionality is the coefficient of drag C_D.

C_D varies with the Reynold's number (Re) of the flow

$$Re = \frac{uD}{\nu} \quad (2)$$

where ν is the kinematic viscosity of the fluid, and D is the diameter of the plate. The C_D for a flat disc normal to a steady flow at high Re has been found to be 1.17 [10, Ch. 7.6]. However, Stokes found that the C_D for an object oscillating in a fluid is greater than that for the same object moving at a steady rate [11].

In oscillatory motion, the inertial force F_M is the force caused by the surrounding fluid accelerating with, or deflecting around, a heave plate. F_M is proportional to the acceleration of the heave plate $\dot{u}$. The added mass can be normalized by a representative mass M related to the heave plate geometry. The ratio of the added mass to the representative mass is called the coefficient of added mass C_M. In this paper, the representative mass will be taken as the theoretical added mass of a disc oriented normal to a flow with diameter equal to that of the heave plate. For clarity, the mass (and inertia) of the actual heave plate will be considered separately from the hydrodynamic added mass.

Manuscript received December 14, 2016; revised July 27, 2017; accepted October 6, 2017. Date of publication November 3, 2017; date of current version October 11, 2018. This work was supported by the Naval Facilities Engineering Command. *(Corresponding author: Adam Brown).*

Associate Editor: B. Buckham.

A. Brown and J. Thomson are with the Applied Physics Laboratory, University of Washington, Seattle, WA 98105 USA (e-mail: brownapl@uw.edu; jthomson@apl.uw.edu).

C. Rusch is with the University of Washington, Seattle, WA 98105 USA (e-mail: curusch@uw.edu).

Digital Object Identifier 10.1109/JOE.2017.2762258

The theoretical added mass of a flat plate can be derived analytically using potential flow as $M = \rho D^3/3$, where D is the diameter of the flat plate [12, Sec. 102, Ch. 6]. Thus, C_M can be defined as the ratio of the measured added mass to the theoretical added mass of a flat plate with equal diameter. The potential flow derivation of the theoretical added mass is directionally symmetric, meaning that the added mass of a submerged shape along a fixed axis does not depend on the direction of motion along that axis [13, §4.14]. This finding does not necessarily hold for real systems, especially in rotational (vortical) flows that violate potential flow assumptions. Although the true velocity field around a heave plate is rotational, the theoretical added mass does provide a reference against which the actual added mass can be normalized. This method of normalization has been used by several authors including Lake *et al.* [6], Garrido-Mendoza *et al.* [14], and Tao and Dray [15].

For scaling purposes, oscillatory hydrodynamic coefficients are often related to the nondimensional Keulegan–Carpenter number (KC), which describes the relative importance of drag forces compared to inertial forces [9], [16, §8.3.5]. These scalings use a characteristic velocity $u \sim a(2\pi f)$, and a characteristic acceleration $\dot{u} \sim a(2\pi f)^2$, where a is the oscillation amplitude and f is the oscillation frequency. After simplification, KC is only dependent on a and a characteristic length, taken as the heave plate diameter D as follows:

$$\mathrm{KC} = \frac{2\pi a}{D}. \tag{3}$$

The nondimensional frequency number β, which is also known as the Roshko number Ro, is derived as the product of Re and the Strouhal number St [17] as follows:

$$\beta = \frac{D^2 f}{\nu}. \tag{4}$$

It can be used as an independent parameter for frequency-dependent oscillatory processes in fluids of varying kinematic viscosity ν. Although it is often mentioned in the heave plate literature for oil and natural gas, β is not typically used as an independent parameter. Rather, all tests are conducted at a set β to reduce the effect of frequency dependence in added mass [7], [14].

In the work that follows, the Morison equation is applied to two sets of experiments, and C_D and C_M are determined for various heave plate designs. The results are scaled using Re, KC, and β. The results are discussed relative to previous work, which is reviewed in Section I-A.

A. Literature Review

Keulegan and Carpenter studied the force on a 2-D cylinder and a flat plate imparted by an oscillating flow of water in a seiche tank [9]. They used a Fourier decomposition of the observed load to calculate the values of C_M and C_D that yield a best fit of the Morison equation to the recorded force. They also quantified the difference between the measured force and the force predicted by the Morison equation as ΔR. The Morison equation produced a reasonable approximation of the observed force for the flat plate; however, the ΔR was significant and its form varied depending on KC. Keulegan and Carpenter attribute the error in the Morison estimate to eddy shedding. Dye injection tests were performed to visualize the types of eddies being shed.

Two other pertinent findings from other authors are discussed by Keulegan and Carpenter. First, Morison *et al.* found that both C_M and C_D for an object in an oscillatory flow will vary significantly from the values predicted by theory (in the case of C_M) and steady flow experimentation (in the case of C_D) [8].

Second, Basset found that the force on an object moving through a fluid depends not only on the current motion of the object, but also on the history of the motion of both the object and the fluid [18]. The history force, which is also known as the Basset force, modifies the standard added mass term provided in (1). However, the accurate calculation of the Basset force is challenging, as it requires a detailed knowledge of the current state and history of the flow field surrounding the object. For this reason, it is often neglected.

Heave plates have primarily been used to stabilize the motion of buoys and offshore structures. Cavaleri and Mollo-Christensen attached a small heave plate to a spar-type sensor buoy deployed in the Mediterranean [19]. Heave plates were first installed on spar-type drilling platforms in the late 1990s, and proved to be an effective means of reducing the response of offshore platforms to surface waves [6]. Wang *et al.* provide an overview of the design practices for spar platforms [20]. As oil and natural gas extraction moved into deeper, more energetic waters, heave plates became more widely accepted and relied upon; understanding their hydrodynamics became critical to predicting the response of concept platforms prior to their fabrication. A body of work has since developed considering the application of heave plates for motion reduction of offshore structures.

If the motion of an offshore structure is modeled as a linear spring mass damper, then the hydrodynamic performance of an attached heave plate can be described in terms of a damping ratio [21, Ch. 7.1.4]. The damping ratio is determined by examining the decay of a perturbation. Damping ratios can be used to develop response amplitude operators that describe the response of a structure to wave excitation at varying frequency.

It is also common to model the hydrodynamic loads on a heave plate using the Morison equation. The performance of the heave plate can then be quantified by C_M and C_D [7], [22]–[24]. Several studies have attempted to identify design parameters that affect the hydrodynamic performance of flat heave plates. For instance, drag is produced, in part, by the creation of vortices as water flows around sharp edges, and thus, the drag coefficient of a heave plate is dependent on the ratio of edge length to surface area, the thickness of the plate, and the shape of the edges.

The modes of vortex generation have been examined in detail by several authors. The particle image velocimetry and numerical studies of Lake *et al.* and Tao *et al.* have attempted to quantify the relation of plate thickness to vortex strength at a given KC. It was found that thinner plates generate stronger vortices, increasing the C_D of the plate [6], [22], [23], [25]. Rosvoll's thesis focuses on the use of CFD to estimate C_D and C_M for a plate oscillating with a small KC number near the

seabed [26]. Garrido-Mendoza *et al.* consider the changes in vortex generation of a heave plate oscillating in close proximity to the free surface and the bottom [14]. It was found that C_M and C_D increase when the oscillation approaches either the free surface or the seabed due to the intensification of spatially constrained vortices.

Shen *et al.* considered variations on the shape of the heave plate's edges [27]. Edge chamfers of varying size and angle were considered, and the effect on hydrodynamic performance was calculated. It was found that C_M and C_D are reduced as chamfer size increases, thus sharp edges result in a heave plate with the most drag and added mass.

The total edge length over which vortices form can be increased by adding perforations to heave plates, and this has been investigated as a means of increasing the damping of plates without changing their planform area [15], [24], [28]–[31]. In 2000, Downie *et al.* published the results of an experimental study in which the response of a spar was measured when subjected to varying incident waves. The spar was fitted with four heave plates of varying porosity. They found that the response of the spar was reduced most using solid heave plates due to the significant differences in the C_M of porous and solid heave plates. Solid heave plates accelerate significantly more water as they oscillate, which reduces the natural frequency of the spar. The frequency of the incoming waves was thus too high to excite the combined mass of the spar and water. However, it is also important to note that the porous plates more effectively reduced the response of the spar when the frequency of the incident waves approached the spar's natural frequency.

Molin used an analytical approach to consider an infinite number of stacked porous heave plates [29]. The effect of varying the spacing of the heave plates was considered, and the relative distance between the stacked plates was defined as the distance between the plates divided by the radius of the plates. Molin's approach only considers the drag associated with flow through the holes of a porous disk; the drag produced due to flow separation at the exterior edge of the plate was not considered. It was found that for flows with a KC number below one, C_D can greatly be increased by adding porosity. However, the benefit of porosity is reduced as the KC of the flow approaches and exceeds one. Increasing the relative spacing of the stacked plates from one to five only increased the per plate damping by 40%, and thus Molin advocated for many plates closely spaced. This conclusion has since been revised by Tao *et al.*, where it is shown that depending on the KC number of the oscillation, there exists a critical distance where the individual heave plates can be treated as independent [22]. It is at this distance that multiple heave plates should be stacked, as the added benefit of each additional heave plate is maximized. Performing a similar study, Sudhakar *et al.* found that above a relative spacing of 0.8, the heave plates could be considered independent [32].

Testing several configurations of heave plates on a model deep draft multispar platform, Li *et al.* found that stacking heave plates did not always reduce system response in near resonant conditions [33]. In the free decay tests, C_D and C_M were greatest when the heave plate was located at the top of the spar near the free surface. Although counterintuitive, this result supports the previously discussed experimental results of Garrido-Mendoza *et al.* who found that proximity to the free surface increases the strength of the generated vortices [14]. Still, the spar with a single heave plate located in deep water demonstrated the least response to an incoming wave field.

Added mass can dominate the dynamics of a heave plate, and for some WEC systems this may be desirable. For example, An and Faltinsen found that perforation at any scale reduced the C_M of the heave plate [24]. Porous heave plates effectively reduce the resonant response of systems, and may be of use in survival situations for WECs. However, most WECs employ heave plates as a relatively stationary body against which the PTO can push and pull. It is the inertia of the added mass (and the plate itself) that reduces the response of the heave plate to the reactionary forces of the PTO. Thus, in most cases, it will be desirable to maximize the C_M of the heave plate.

Li *et al.* performed a comprehensive analysis in which they systematically tested the effect of key design parameters on hydrodynamic performance at varying KC and β [7]. The varied parameters included distance from the free surface, plate porosity, porous hole size, plate thickness-to-width ratio, edge shape, and the spacing of stacked plates. It was found that C_D decreases as KC increases to a value of 0.6, above which the C_D remains roughly constant at 6.0. It was also found that increasing perforation ratio increases the coefficient of drag at low KC, and reduces C_M at all values of KC. The hole size used to make the porous plates was found to have little effect on either C_M or C_D. Both C_M and C_D increased with decreasing plate thickness, and both C_M and C_D were maximized by the presence of sharp plate edges. However, the edge shape effect is minor, and it is likely that sharp edges will rapidly become blunted by fouling in the marine environment. It was found that C_M and C_D primarily varied with KC. C_M was weakly dependent on β, increasing slightly as β increases, while C_D was found to be independent of β. However, this finding deserves further investigation, as the dependence of C_D on the velocity proportional Re suggests that oscillation frequency should have an effect on C_D.

The existing heave plate literature provides a strong base for further research on the use of heave plates for wave energy conversion. However, heave plates used for oil and natural gas platforms are much larger than those used for wave energy conversion. Thus, the mode of operation and the range of experimental variables tested for platform heave plates tend to lie outside the range of interest for wave energy conversion. In particular, poor characterization of heave plate hydrodynamic behavior likely has contributed to model-data disagreements in recent WEC prototype testing [5], [34].

Furthermore, WECs may benefit from more complicated heave plate geometries. For example, WECs may use a flexible tether to attach a heave plate at depth to a PTO located near the surface. Flexible tethers can be damaged by repeated loading and unloading or snap loading. A heave plate with asymmetric shape and behavior that falls through the water more easily than it is raised may reduce how often its tether is unloaded and reloaded [35], [36]. In 2014, Ebner used various techniques to assist Oscilla Power, Seattle, WA, USA, in determining the

Fig. 1. Oscillator test apparatus, which is mounted to the edge of a dock and uses a linear actuator to force submerged heave plate oscillations with a pushrod.

added mass and drag for various heave plate concepts, some of which were asymmetric. The experiments performed include model scale WEC tests of wave induced and free-decay motion, as well as tow-tank tests to determine drag and added mass [4].

II. Methods

A. Oscillator

The Oscillator is an experimental testing facility at the dock of the Applied Physics Laboratory at the University of Washington. The Oscillator uses a servomotor-driven belt-and-carriage linear actuator to force small-scale heave plates (30.5-cm diameter) vertically through the water column. The system is capable of producing near sinusoidal oscillations with a peak-to-peak height up to 1.25 m (see Fig. 1). The design is similar to devices that have been used by other authors to determine hydrodynamic coefficients for heave plates and other floating structures [7], [37].

Heave plates are mounted to the bottom of a pushrod 0.9 m below the water surface, and the pushrod is then driven by the actuator carriage. A 1300 N S-beam load cell is used to measure the force driving the heave plate and pushrod. The output from the servomotor's high-accuracy analog resolver (rotary position) is converted to provide the linear position of the carriage. Heave plate velocity and acceleration are obtained through differentiation of the recorded linear position.

TABLE I
Combinations of Amplitude and Period Tested for Each Heave Plate on the Oscillator

a, cm	KC	T, s	0.25	0.5	1.0	2.0	4.0
		β	$3.7e^5$	$1.9e^5$	$9.3e^4$	$4.6e^4$	$2.3e^4$
0.5	0.10		X				
1.25	0.26		X	X			
2.5	0.52			X			
5.0	1.03				X	X	
7.5	1.55				X	X	
10.0	2.06				X	X	
15.0	3.09					X	X
20.0	4.12					X	X
25.0	5.15						X
30.0	6.18						X
35.0	7.21						X

The commanded oscillations are passed to the Oscillator by an analog input to the motor controller. The voltage of the input signal corresponds to the desired position of the actuator carriage. The signal is generated using Labview and the analog output channel of a USB data acquisition system. Within the same Labview program, the actual motion and the resulting load on the heave plate are recorded at 200 Hz.

The motor controller uses a proportional-integral-derivative (PID) algorithm to match the actual position of the carriage to the commanded position. The PID gains were manually tuned before testing to minimize the error between desired and actual position while maintaining smooth and stable operation. The error between the desired sinusoidal motion and the actual recorded position depends on the period and amplitude of the oscillation and the gains of the motor controller. Motion is ramped to full amplitude over two oscillations, and before analysis, the first five oscillations are cropped from the data to minimize the impact of transient behavior.

Position and force samples are recorded simultaneously throughout the cycle of each wave. The number of samples per cycle is determined by the combination of oscillation period T and sampling frequency f_s as $N_{\text{samples}} = f_s T$.

Monochromatic oscillations with amplitudes varying between 0.5 and 35 cm were tested with periods ranging between 0.25 and 4 s (see Table I). Each combination of test parameters was repeated for the following four different heave plate variations:

1) a 30.5-cm diameter flat plate;
2) a 30.5-cm diameter flat plate with a 10.2-cm central hole;
3) a hexagonal conic with approximately 45° sidewalls, 16.1-cm outer edge lengths, and a flat bottom with 5.2-cm edge lengths;
4) the same hexagonal conic with the bottom removed.

As built, the planform area of the closed hexagonal conic was 4% less than the area of the flat plate, and the central hole of the hexagonal conic was 6% larger than the hole in the flat plate.

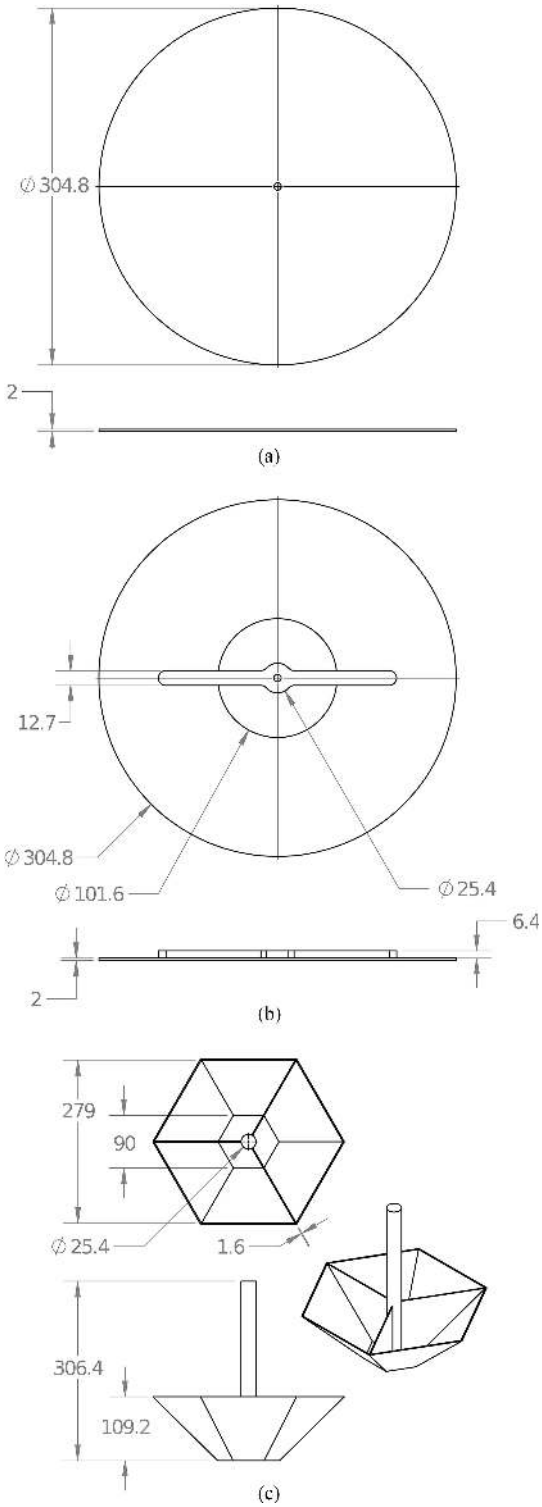

Fig. 2. Heave plates used on the Oscillator: (a) flat plate, (b) flat plate with central hole, and (c) hexagonal conic, tested with the lower hole open and closed. All dimensions are in units of millimeter.

The conics were tested with their wide sides up. Dimensioned drawings for these heave plates are provided in Fig. 2.

Testing on the Oscillator is conducted by entering an array of desired combinations of amplitude and period. After the test parameters have been specified, the Oscillator begins by finding its home position. This position is located at the maximum vertical displacement of the actuator carriage. From this position, the oscillator lowers the heave plate to its operational depth in the water column (90 cm). This depth is specified as the zero position, which is the average depth of the heave plate as it moves through the commanded sinusoidal motion. Once the zero position is reached, data collection begins. The heave plate remains stationary for 30 s before and after the full amplitude oscillations; this allows for the calculation of the wet weight of the heave plate. Oscillations are ramped to and from full amplitude over two wave periods. The position of the actuator carriage and the tension in the thrust rod are continuously recorded. About 200 full amplitude oscillations are recorded when the commanded period is between 0.25 and 1 s, 150 oscillations are recorded when the period is 2 s, and 100 oscillations are recorded when the period is 4 s. The high number of repeated oscillations is useful to minimize the effects of boat wakes and small wind waves, which are occasionally present at the dockside testing site. Upon completion, the recorded data are written to a file, and testing automatically begins for the next combination of amplitude and period. A full set of tests, as shown in Table I, takes approximately 4 h for each heave plate.

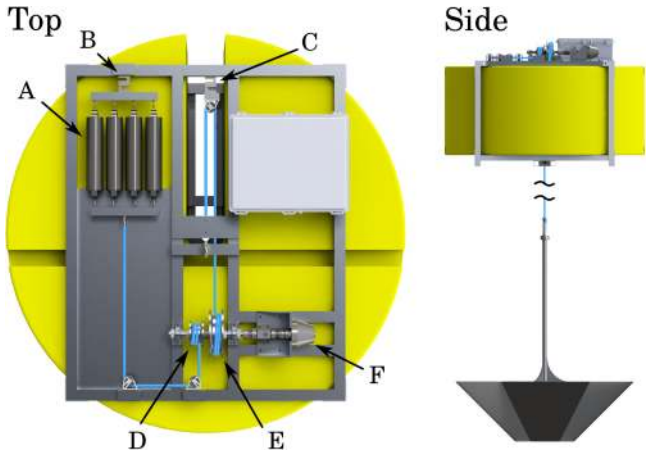

Fig. 3. miniWEC is a floating point absorber that uses the rotation of a spring loaded spindle to produce power. A heave plate is tethered to the spindle opposing the springs such that the motion of the waves causes the spindle to oscillate around the equilibrium point. The labeled components are A) the extension springs, B) the spring load cell, C) the heave plate tether load cell, D) the spring spindle, E) The tether load cell, and F) the rotary dashpot.

B. Mini Wave Energy Converter (miniWEC)

The miniWEC is a 1.8-m diameter, point-absorbing WEC, designed and built by the University of Washington Applied Physics Laboratory, Seattle, WA, USA, that provides a means of studying the unconstrained hydrodynamic behavior of heave plates used for wave energy conversion at the field scale (see Fig. 3). The miniWEC is comprised of a heave plate suspended below a surface float by a flexible tether. On the surface float, the tether is wrapped around a spindle. When the float moves relative to the heave plate, a moment is imparted on the spindle that is countered by a second line attached to a bank of extension springs. The extension spring spindle is one half the diameter

of the heave plate tether spindle, such that the line travel of the heave plate tether is double that of the spring line and the static spring force is twice the wet weight of the heave plate. The weight of the heave plate causes the heave plate tether spindle to unwind, stretching the springs until the system reaches equilibrium. The incident waves induce motion in the float, which causes the spindle to oscillate about the equilibrium point. Energy from the spindle shaft was dissipated using a rotary dashpot. The torque curve of the dashpot is velocity proportional, similar to that of a gearbox and generator. A controllable PTO will be added to the miniWEC in future experiments. Many systems that are dynamically similar to the miniWEC have been proposed and studied [38]–[40]. AquaHarmonics, Portland, OR, USA, Fred Olson, Oslo, Norway, and Oscilla Power, Seattle, WA, USA, are just a few examples of companies attempting to develop systems that are conceptually similar to the miniWEC [34], [41].

The miniWEC measures and records the float orientation and acceleration, heave plate tether tension, return spring tension, spindle position, and waterline position simultaneously at 50 Hz. The data acquisition system onboard the miniWEC surface float uses a National Instruments cRIO-9030. A wireless network is used to communicate with the miniWEC during operation (for data and fault monitoring).

Two heave plates, geometrically similar to the Oscillator heave plates, were tested using the miniWEC. The first heave plate is a 1.5-m diameter standard flat plate with a 0.5 m central hole, and the second is a hexagonal conic with approximately the same planform area as the flat plate and a central hole of approximately equal area (see Fig. 4). Testing was conducted for each heave plate with the central hole left open, and then tests were repeated after covering the hole with a thin flat plate. The weight of the heave plates was designed to stretch the extension springs approximately 30 cm to a neutral position at half of their maximum extension. The mass of the flat heave plate is 275.5 kg, and the mass of the hexagonal conic heave plate is 258.5 kg.

A Lowell MAT-1 stand-alone submersible data-logging inertial measurement unit (IMU) was attached to the heave plates and measured their motion at 64 Hz. A Nortek Vector ADV measuring both hydrostatic pressure and relative water velocity at 16 Hz was also mounted to the heave plate. During testing, the IMU suffered a seal failure and flooded, therefore heave plate acceleration is only available for the two flat plate tests.

On April 5, 2016, the R/V Jack Robertson was used to deploy and monitor the miniWEC on Lake Washington, near the University of Washington, Seattle, WA, USA. The miniWEC was released upwind and allowed to freely drift downwind from South to North. Each free-drifting data collection run lasted approximately 1 h. At the end of each run, the miniWEC was recovered, and the heave plate configuration was changed. The miniWEC was then moved back to its starting position and released for the next test run. Due to calm conditions on the day of deployment, it was necessary to excite the miniWEC with wakes from the research vessel (see Fig. 5). Although wake excitation is insufficient to determine the overall performance of the miniWEC, the motion induced in the heave plates can be used to determine hydrodynamic coefficients.

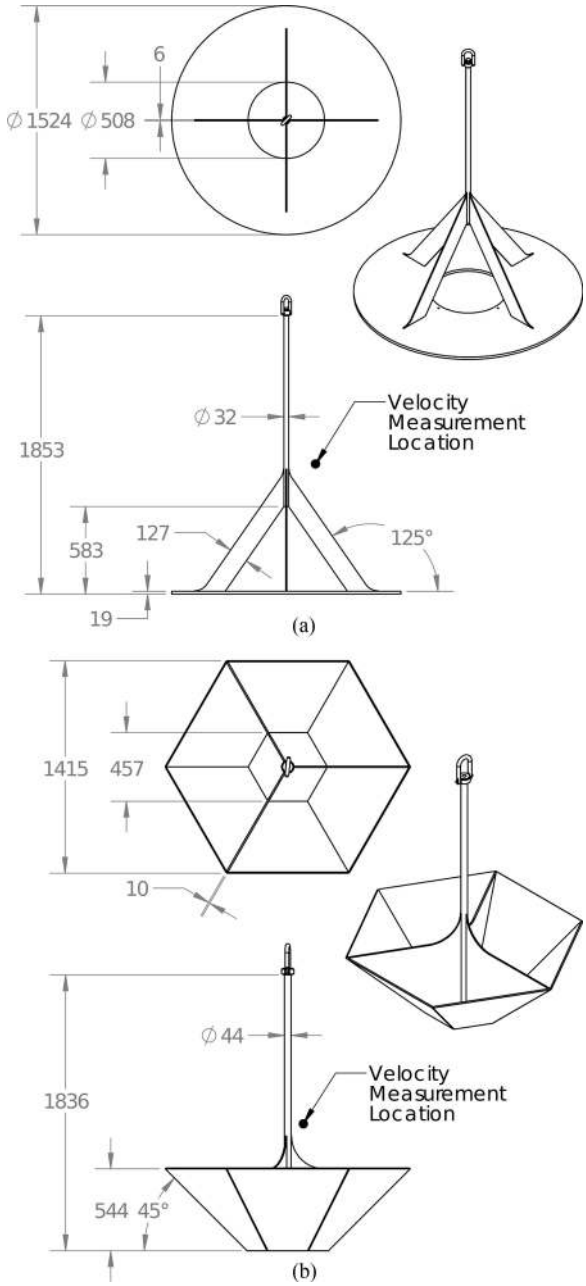

Fig. 4. Heave plates tested using the miniWEC: (a) flat plate and (b) hexagonal conic. Both heave plates were tested with their lower holes open and closed. All dimensions are in units of centimeter.

The velocity of the water relative to the heave plate was measured by the Nortek Vector ADV at a location near the centerline of the heave plate, approximately 0.8 m above the bottom plane of each heave plate (see Fig. 4). During postprocessing, this velocity is filtered and differentiated to provide an approximation of heave plate acceleration. The body of the Nortek Vector was mounted to the bottom plate of the flat heave plate (see Fig. 5), and inside the bell of the hexagonal conic heave plate. Water pressure is measured at a port on the body of the Nortek Vector; this is used as a measure of instantaneous depth, and thus position, relative to mean sea level. Heave plate position calculated from water pressure is then filtered and twice differentiated to

Fig. 5. Left: The miniWEC and flat heave plate on the work deck of the R/V Robertson before deployment. Right: The hexagonal conic heave plate during transit to the test site. Bottom: The miniWEC was deployed on Lake Washington. Due to calm conditions, boat wake was used to excite the surface float.

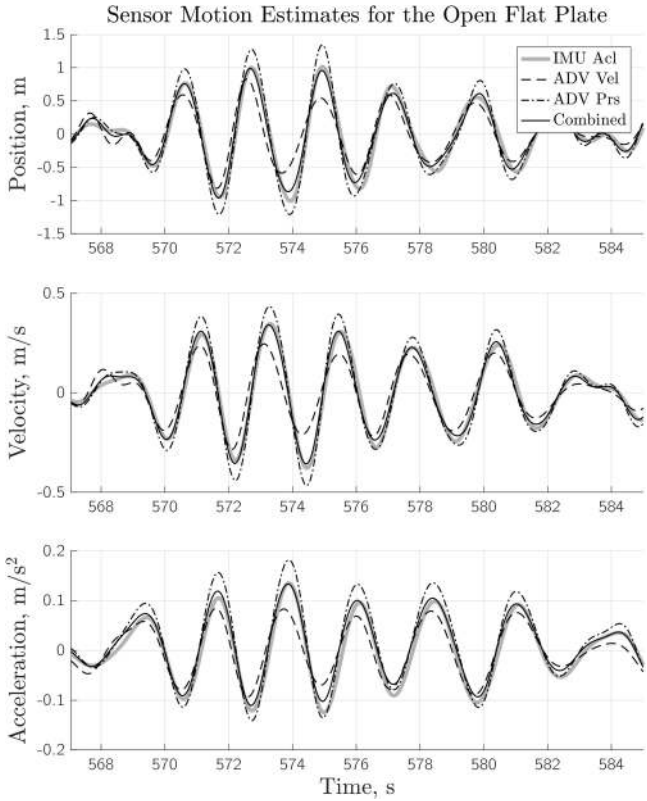

Fig. 6. Estimates of heave plate motion derived from the three sensors mounted to the open flat plate. The sensors were a Lowell MAT-1 IMU measuring heave plate acceleration, and a Nortek Vector ADV measuring water pressure and velocity.

provide an independent approximation of velocity and acceleration. For the two flat plate tests where IMU data are available, the raw vertical acceleration of the heave plate is filtered and integrated to yield another estimate of heave plate velocity and position.

The motion of the heave plate calculated from the acceleration of the IMU is considered more accurate than either of the Nortek Vector measurements. The IMU is measuring the actual motion of the heave plate, whereas both the velocity and pressure measurements from the Nortek Vector are influenced by the motion of the surrounding water. The ADV is not measuring the true free-stream velocity of the heave plate through the water, as the measurement point is located relatively near the upper plane of the heave plate, and the measurement of the pressure sensor is affected by dynamic variations in the pressure field surrounding the heave plate as it moves through the water. For the flat plate tests, all three sensors were operational, and the IMU data provide a calibration of the estimates of heave plate motion derived from ADV water velocity (a_{wv}) and pressure (a_{prs}). Fig. 6 shows that all three estimates are similar. However, the motion of the heave plate estimated from ADV water velocity is slightly less than the motion estimated from the acceleration of the IMU, and the motion derived from water pressure is slightly greater than the estimate from the IMU.

As a postprocessing step, the pressure and water velocity based estimates of motion are averaged according to

$$\bar{a} = W_{\mathrm{wv}} a_{\mathrm{wv}} + W_{\mathrm{prs}} a_{\mathrm{prs}}. \tag{5}$$

TABLE II
WEIGHTING COEFFICIENTS FOR ESTIMATES OF HEAVE PLATE POSITION, VELOCITY, AND ACCELERATION DERIVED FROM THE MEASUREMENTS OF ADV WATER VELOCITY AND PRESSURE THAT MOST ACCURATELY REPRODUCE THE MOTION IMU MOTION ESTIMATE

	W_{wv}	W_{prs}
Position	0.231	0.659
Velocity	0.128	0.744
Acceleration	0.267	0.629

The optimal averaging weights W_{wv} and W_{prs} are determined using the least squares method, such that the error between the IMU acceleration and the average acceleration ($\bar{a}$) is minimized. A detailed formulation of the least squares method can be found in [42, Ch. 3.3.1]. The averaging is shown only for acceleration in (5); however, this method was also used to find averaging weights for velocity, and position.

The optimal weighting coefficients, which were used to estimate the motion of the hexagonal conic heave plates are shown in Table II. The acceleration recorded by the IMU was used directly to estimate the motion of the flat heave plates. The estimate of motion from the combined velocity and pressure measurements is also plotted in Fig. 6, and shows a good fit to the motion derived from IMU acceleration. The sensitivity of the

calculated hydrodynamic coefficients to errors in the estimated motion is presented in the appendix.

The cRIO, IMU, and Vector ADV were all running on their own clocks, and recording at different frequencies; therefore, the data must be synchronized in postprocessing. Synchronization begins with a gross alignment of corresponding wake signatures in the three data sets. The gross alignment refines the time synchronization to within ± 0.5 s. To further refine the time synchronization, the RMS error of the Morison estimate E_{RMS} is minimized for varying time shifts t_{sync} added to the ADV and IMU clocks according to the following equation:

$$E_{\mathrm{RMS}} = \sqrt{\frac{1}{n}\sum_{i=1}^{n}(F_H(t_i) - F_{\mathrm{Mor}}(t_i + t_{\mathrm{sync}}))^2}. \quad (6)$$

Through iteration, the optimal values of t_{sync} were found for each test to an accuracy of ± 0.01 s. The sensitivity of the analysis to time synchronization is also discussed in the appendix.

Equation (6) assumes that the two data sets were sampled at corresponding times. As this is not true for the miniWEC data, the higher sampling rates are interpolated to match the slower data. For the flat plate tests, linear interpolation was used to estimate the heave plate acceleration recorded by the IMU at the moment the cRIO was sampled given a time offset of the clocks equal to t_{sync}. This same method was used to synchronize the cRIO clock to that of the ADV for all four heave plate tests. For the miniWEC tests, only periods of active wake excitation were used for time synchronization and the calculation of hydrodynamic coefficients.

C. Calculation of Hydrodynamic Coefficients

The hydrodynamic force F_H is the force acting on the heave plate due to the motion of the heave plate through the water. The dry weight W and buoyancy B of the heave plate must be subtracted from the recorded force at the load cell F_{LC}. The inertial force due to the acceleration $\dot{u}$ of the heave plate mass m must also be removed from F_{LC}, such that

$$F_H = F_{\mathrm{LC}} - W - B - m\dot{u}. \quad (7)$$

On the Oscillator, the load cell is located between the actuator carriage and the thrust rod, and the weight and inertia of the thrust rod must also be removed from F_{LC}. The displacement of the thrust rod changes with time, and thus B varies in time for Oscillator tests. Buoyancy is constant for the miniWEC tests.

The method of least squares is used to calculate the values of C_D and C_M that produce a best fit of F_{Mor} to the experimentally determined F_H. Several authors have used this method, or variations on this method, to determine coefficients of added mass, drag, and damping [6], [14], [15], [43]. If this method is applied to a continuous time series of data spanning multiple oscillations, the calculated constant coefficients produce the best fit of the Morison equation to the observed hydrodynamic force.

The Morison equation with constant coefficients provides a simple estimate of the hydrodynamic forces acting on a heave plate. However, this method will always produce a symmetric solution, in which sinusoidal motion has the same force variation for the upstroke and the downstroke. For asymmetrically shaped heave plates, this limitation may lead to increased error. To quantify asymmetry, instantaneous coefficients of drag and added mass were calculated for every data point in the data set. The instantaneous coefficients will be denoted by $\widetilde{C_M}$ and $\widetilde{C_D}$, and the Morison force estimate produced using the instantaneous coefficients will be denoted by $\widetilde{F_{\mathrm{Mor}}}$. Although termed "instantaneous," these coefficients were actually calculated within a small rolling window of data, and ascribed to the central point of that window. The window used for this study spanned approximately $\pm 90^\circ$ of oscillation phase. For the Oscillator tests, sampling occurred at consistent phases of the oscillation, thus it was also possible to determine the mean values of $\widetilde{C_M}$ and $\widetilde{C_D}$ as a function of oscillation phase.

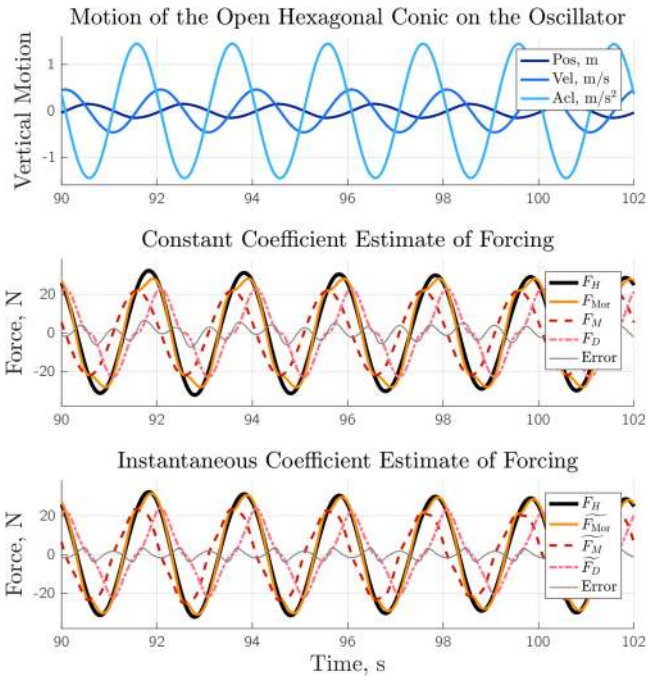

Fig. 7. Top: Oscillator motion data for the open hexagonal conic undergoing an oscillation with a 15.0 cm amplitude and a 2.0 s period. Middle: The force predicted by the Morison Equation using constant coefficients and the components of that force. Bottom: The force predicted by the Morison Equation using instantaneous coefficients and the components of that force.

III. Results

A. Time Series

A representative segment of time series data from the Oscillator is shown in Fig. 7. The open hexagonal conic was forced through an oscillation with an amplitude of 15.0 cm and a period of 2.0 s. The weight, dynamic buoyancy, and inertia of the rod and heave plate have been subtracted from the recorded force, which has been lowpass filtered. For all tests of the Oscillator and miniWEC, the cutoff frequency was set at approximately $3/T$, where T is either the commanded period of the oscillation. Heave plate motion was filtered after each integration or differentiation. Detailed filter parameters are shown for both the Oscillator and miniWEC in Table III.

Using the motion shown in the top panel of Fig. 7, constant coefficients are calculated and used to reconstruct the forces on

TABLE III
PARAMETERS FOR THE FILTERS USED ON EACH SIGNAL FOR THE MINIWEC AND OSCILLATOR EXPERIMENTS

Platform	Signal	Highpass		Lowpass	
		order	f_{cut}	order	f_{cut}
Oscillator	All	4	$1/(15T)$	6	$3/T$
miniWEC	Force	4	$1/60$	6	4
	Motion	4	$1/15$	6	1.5

All filters were zero-phase Chebyshev Type II of the given order with a stopband 50 dB below the passband. For the oscillator, the cutoff frequencies f_{cut} vary with the period of the oscillation T.

the heave plate shown in the middle panel (see Fig. 7). For all cases, the Morison equation with constant coefficients provides a reasonable approximation (F_{Mor}) of the actual forces observed (F_H). However, F_{Mor} tends to underestimate the maxima and minima of F_H by approximately 5–20%. In the bottom panel of Fig. 7, it can be seen that $\widetilde{F_{\mathrm{Mor}}}$ produces a better estimate of the recorded hydrodynamic force, and notably improves the fit at moments of peak forcing.

On the Oscillator, the worst fits of F_{Mor} to F_H occur for tests of small amplitude, low-frequency oscillations. This is likely due to the fact that the amplitude of the hydrodynamic force approaches the ± 3 N friction/noise floor of the load cell (see appendix). All tests approaching the noise floor were omitted from analysis, and all test configurations shown in Table I had a signal-to-noise ratio of 2.5 or greater.

For the small amplitude tests performed on the Oscillator, the relative importance of F_M dominates F_D. However, as the oscillation amplitude increases, the amplitude of the forces quickly equalize for the remainder of the tests. This is because F_D is proportional to the square of heave plate velocity, while F_M is proportional to acceleration. Velocity scales with amplitude and frequency, and acceleration scales with amplitude and frequency squared. Thus, changes in amplitude have a greater effect on the magnitude of F_D than they do on F_M, because F_D has an amplitude dependence that is effectively quadratic (compared with the linear dependence on amplitude for F_M).

A representative segment of time series data from the miniWEC is shown in Fig. 8. The data are from the test of the hexagonal conic with the central hole closed. Both F_{Mor} and $\widetilde{F_{\mathrm{Mor}}}$ provide excellent approximations of the measured F_H. As with the Oscillator results, the miniWEC results with constant coefficients tend to underestimate the maxima and minima of the measured force, while overestimating the low amplitude forces that occur near the end of the wake excitation.

For all of the heave plate configurations tested using the miniWEC, added mass F_M tends to dominate drag F_D. This is likely due to the small amplitude heave plate oscillation induced by the boat wake. For longer period, larger amplitude waves, greater heave plate velocities will increase the relative importance of F_D.

B. Constant Hydrodynamic Coefficients

All of the constant coefficient results from both the Oscillator and miniWEC tests have been combined in Fig. 9 and presented

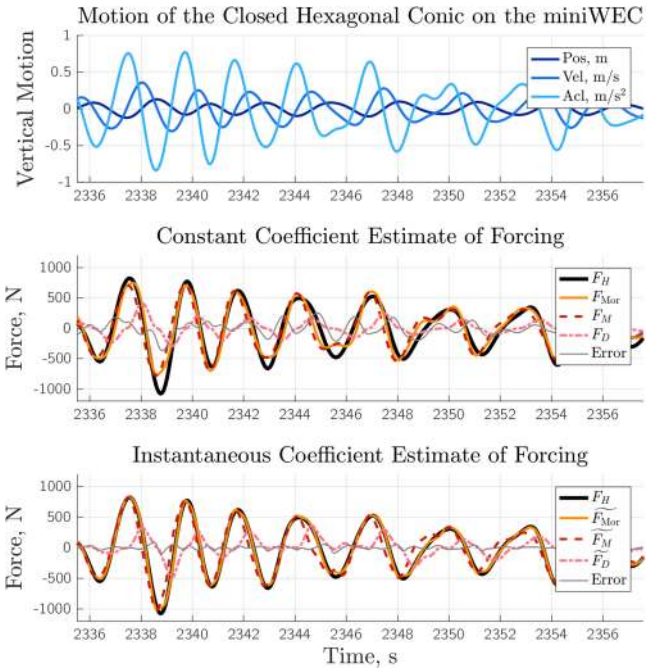

Fig. 8. Motion and force data for the closed hexagonal conic heave plate tested using the miniWEC. The motion and forces are typical of excitation with boat wake. Both the constant and the instantaneous Morison coefficient approximations provide a good fit to the recorded force.

as a function of the nondimensional parameters KC, β, and the RMS of Re.

The constant drag coefficients vary with both KC and Re. Although there is a strong dependence on KC across the various tests, C_D does not appear to scale with KC between the Oscillator results and the miniWEC results. By contrast, it appears that Oscillator tests are converging to the miniWEC values as Re_{RMS} increases. The Oscillator data show some variation in C_D for different heave plate shapes at low Re, but that variation diminishes as Re and KC increase.

For all four of the heave plates tested on the Oscillator, C_D at high Re_{RMS} falls to a value between 2.0 to 3.5. This is somewhat higher than the value of 1.17 for a for a flat disc normal to a steady flow at high Re [10, Ch. 7.6]. However, it is also expected that the C_D for oscillatory flow will be greater than that for an equivalent steady flow [11].

The constant added mass coefficients vary with both KC and β, with β appearing to provide the best scaling between the experiments. For the Oscillator results, C_M appears nearly constant at its minimum value ~ 1 until a KC of approximately 0.5 is reached, where C_M begins to increase with KC. The increase is most notable for the closed flat plate.

For the miniWEC data presented in Table IV, the closed hexagonal conic has the greatest added mass coefficient. However, all of the added mass coefficients for the miniWEC heave plates are below the theoretical value of added mass. For all tests conducted with both the Oscillator and miniWEC, the heave plates with a central hole have added mass coefficients less than their closed counterparts.

The miniWEC and Oscillator results have been plotted with the results of several other authors. The Oscillator results compare well with the prior literature. The drag coefficients

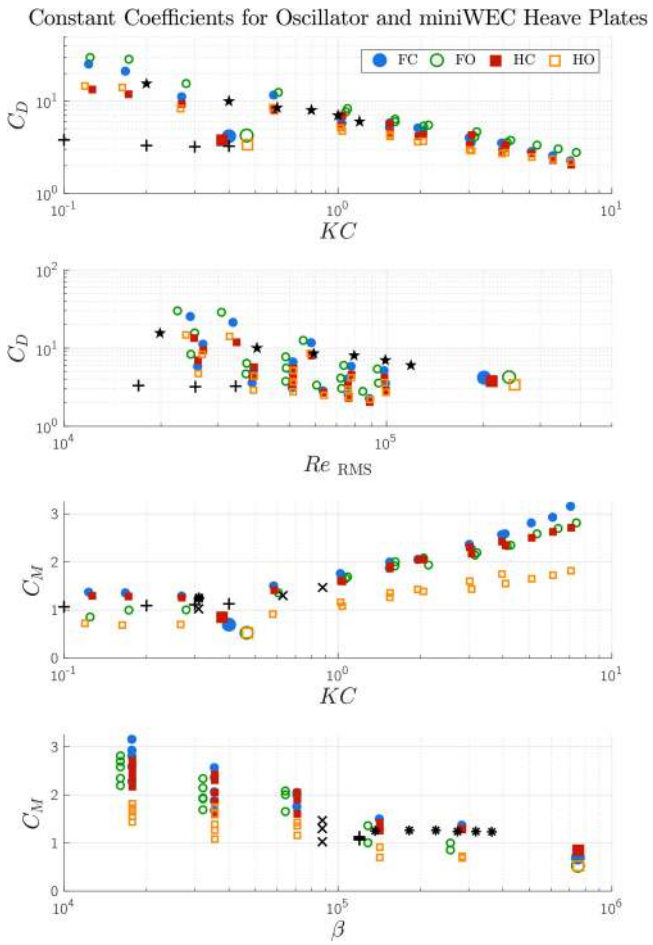

Fig. 9. Constant coefficients for all Oscillator and miniWEC tests. For all panels, the small markers are results from the Oscillator, and the large markers are from the miniWEC. FC = closed flat plate; FO = open flat plate; HC = closed hexagonal conic; and HO = open hexagonal conic. For comparison, values from [6] are shown as (+), values from [14] are shown as (×), values from [43] are shown as (∗), and values from [15] are shown as (⋆).

TABLE IV
CONSTANT AND DIRECTIONAL C_M AND C_D FOR THE FOUR MINIWEC HEAVE PLATES

Heave plate	C_M			C_D		
	Cnst	Up	Down	Cnst	Up	Down
Flat closed	0.62	0.61	0.63	3.9	3.9	3.9
Flat open	0.44	0.43	0.45	4.0	3.9	4.0
Hex closed	0.79	0.77	0.80	3.5	3.8	3.2
Hex open	0.44	0.43	0.46	3.5	3.6	3.5

calculated for the miniWEC heave plates appear to fit the trend of the Oscillator experiments when plotted against Re_{RMS}. However, plotted against KC, the miniWEC results lie below the Oscillator results. It is interesting that the C_D results of Lake *et al.* derived from oscillations at very low Re_{RMS} appear to match the values of the miniWEC heave plates when plotted against KC. The miniWEC C_M is less than any of the other results shown, and also below the potential flow solution for a flat disc of equal diameter. This could be related to the unconstrained motion of the miniWEC heave plates, which are free to pitch, roll, and surge. It is possible that the extra degrees

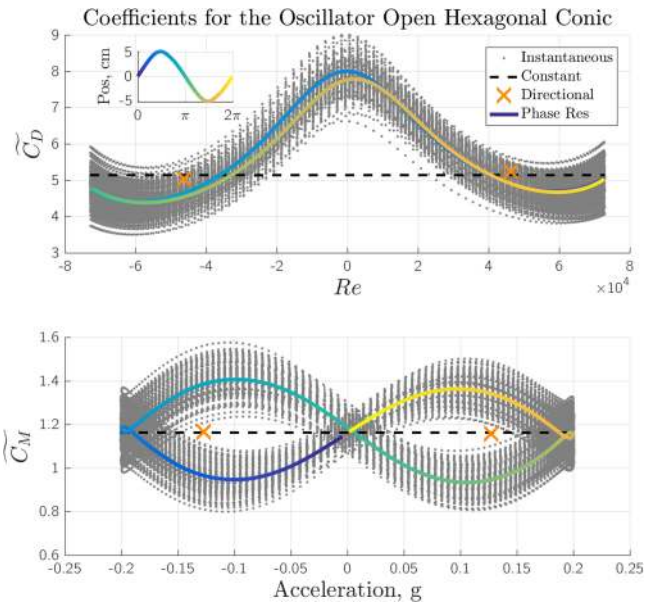

Fig. 10. Instantaneous, constant, directional, and phase-resolved hydrodynamic coefficients are shown for the open hexagonal conic moving through an oscillation of 5-cm amplitude and 1-s period.

of freedom allow the heave plates to shed some of their added mass.

Directional coefficients of added mass and drag were also calculated for both the miniWEC and Oscillator experiments. For drag, an upward directional coefficient is calculated using all data sampled while the heave plate is moving upward, and an upward added mass coefficient is the value derived from all data sampled while the heave plate is accelerating in the upward direction. The downward coefficients are similarly calculated.

The constant and directional coefficient values for each heave plate configuration are shown in Table IV. The closed hexagonal conic shows some directional dependence with a downward C_D of 3.2 and an upward C_D of 3.8. However, none of the other heave plate configurations showed significant directionality of C_D or C_M.

C. Instantaneous Hydrodynamic Coefficients

Plots of $\widetilde{C_D}$ and $\widetilde{C_M}$ versus instantaneous values of Re and acceleration are shown in Figs. 10 and 11. A negative Re indicates downward motion, and a positive Re indicates upward motion; the same convention is used for acceleration. Although the values of $\widetilde{C_D}$ are greater than they would be for a steady flow at equivalent Re, the shape of the $\widetilde{C_D}$ versus Re curve is similar to the expected steady flow curve, with C_D decreasing as Re increases in magnitude.

For the Oscillator example, the instantaneous $\widetilde{C_M}$ are very nearly directionally symmetric (see Fig. 10). However, the value of $\widetilde{C_M}$ varies with the phase of the oscillation, creating the loopy appearance of the instantaneous coefficients. This could be a result of the heave plate oscillation inducing a flow in the surrounding water. The Basset history force term, as discussed in Section I-A, would be needed to fully model the effect of the induced flow. An induced flow would have the effect of advancing the phase of the relative velocity. Consistent with

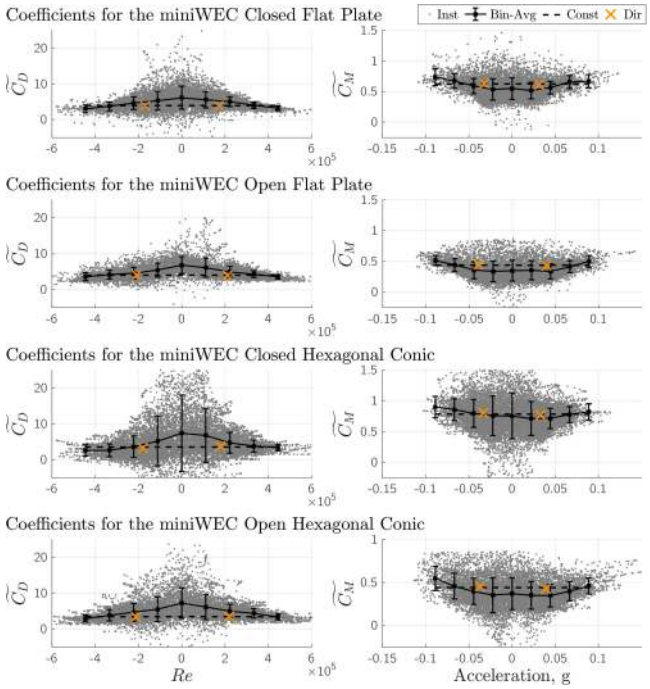

Fig. 11. Instantaneous hydrodynamic coefficients for the four heave plate configurations tested using the miniWEC. Only data points sampled during active wake excitation are shown. Bin averages and standard deviations are shown to highlight directionality and variance.

Fig. 7, advancing the phase of F_D would improve the fit of F_{Mor} to F_H.

Oscillator tests of the open and closed hexagonal conic heave plates do show some hydrodynamic asymmetry in the instantaneous drag coefficients $\widetilde{C_D}$. However, some asymmetry was also seen in $\widetilde{C_D}$ coefficients for the flat plate tests. Thus, a portion of the asymmetry observed in $\widetilde{C_D}$ is likely due to the test configuration and/or induced flow. Turbulent boils were observed on the water surface during some of the large amplitude, high Re tests using the Oscillator. This could indicate that the asymmetry is due to intensification of the turbulent eddies near the free surface. The hydrodynamic force for the low-amplitude, long-period oscillations was on the order of 10 N. For these tests, any minor error in load cell calibration, amplifier drift, or bearing friction could lead to the observed asymmetry in $\widetilde{C_D}$.

Instantaneous coefficient clouds are shown for the miniWEC heave plates in Fig. 11. Bin averages, intended to highlight directionality, are shown for $\widetilde{C_D}$ and $\widetilde{C_M}$ at a given Re and a given acceleration. The markers shown in Fig. 11 are located at the center of each bin, and the bin widths are approximately 111 000 for Re, and 0.022 $\mathrm{m/s^2}$ for acceleration. For the miniWEC heave plates, there is a decrease in $\widetilde{C_D}$ with increasing Re magnitude, similar to the Oscillator results. The flat plates and the open hexagonal conic, show little evidence of asymmetry. The closed hexagonal conic shows some asymmetry of C_D, however C_M remains nearly symmetric.

Directional variation of $\widetilde{C_M}$ is minimal for all four heave plates. The slight reduction in the average added mass coefficient for small amplitude accelerations is likely due to a reduction in the signal-to-noise ratio as the amplitude of the observed motion diminishes.

Unlike the Oscillator tests, $\widetilde{C_D}$ and $\widetilde{C_M}$ for the miniWEC heave plates do not appear to fall into consistent cyclic patterns. Patterns in the miniWEC data may be obscured by the nonmonochromatic and nonstationary nature of the wake excitation. This is compounded by the slow sampling rate of the Nortek vector relative to Oscillator data. Both the ADV and pressure signals were noisy, and the noise contamination in the miniWEC data increases variance in $\widetilde{C_D}$ and $\widetilde{C_M}$. Use of the higher frequency accelerometer data for the flat plate tests substantially reduces the variance of the calculated instantaneous coefficients.

For both the Oscillator and miniWEC data, the least squares solution for constant C_M and C_D most closely matches $\widetilde{C_M}$ and $\widetilde{C_D}$ during periods of peak Morison component forcing. Despite the clear intracycle variations in the instantaneous coefficients, the resulting F_{Mor} provides a reasonable fit to the observed F_H using just the constant coefficients. However, use of the instantaneous coefficients improves the fit of $\widetilde{F_{\mathrm{Mor}}}$ to F_H, which suggests that WEC models may benefit from phase-resolved coefficients of added mass and drag.

IV. Conclusion

Both constant and instantaneous coefficients of drag C_D and added mass C_M are determined from four heave plate shapes at two different scales (lab and field). C_D is dependent on both KC and Re_{RMS}. However, the scaling of C_D from the Oscillator tests to the miniWEC tests appears to be more consistent in Re_{RMS}. C_D for all four heave plates across all tests are greater than the steady flow equivalent, and match well with the prior literature. C_M is dependent on KC and β, and appears to scale with β. The added mass of all four miniWEC heave plates is significantly less than the theoretical value for a flat plate in oscillating flow. This could be due to additional degrees of freedom in the miniWEC heave plate motion. The values of C_M from the Oscillator test match well with prior literature. The lab-scale (Oscillator) results for C_D approach the field-scale (miniWEC) results with increasing Re_{RMS}, and the values of C_M for the lab-scale tests approach the field-scale values with increasing β.

For most of the Oscillator tests, the effect of asymmetric geometry on hydrodynamic asymmetry was marginal; however, the closed hexagonal conic tested on the miniWEC did show a small increase in C_D in the upward direction. The 3-D shape of the closed hexagonal conic elevated the added mass of the heave plate in both the up and down directions.

Results suggest that the Morison equation is a valid description of heave plate hydrodynamics. For both the miniWEC and Oscillator tests, the Morison equation using constant coefficients provides a reasonable fit to the hydrodynamic forces measured during heave plate oscillations. Peak forces are typically underpredicted with a maximum error of approximately 20% and an average error less than 10%. The use of instantaneous coefficients of added mass and drag further improves the Morison estimate of heave plate forcing. This suggests that as the quality

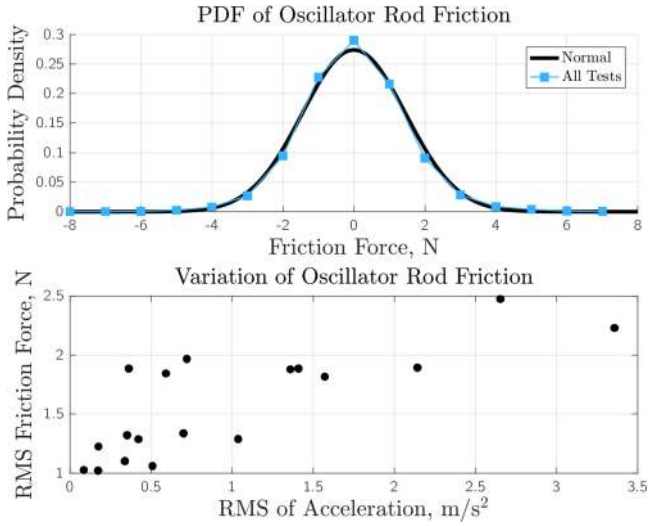

Fig. 12. Top: The probability density function for frictional force in the Oscillator guide bearing is compared to a normal distribution of equal standard deviation ($\sigma = 2.2$ N). Bottom: The RMS of the frictional force is plotted against the RMS of the rod acceleration.

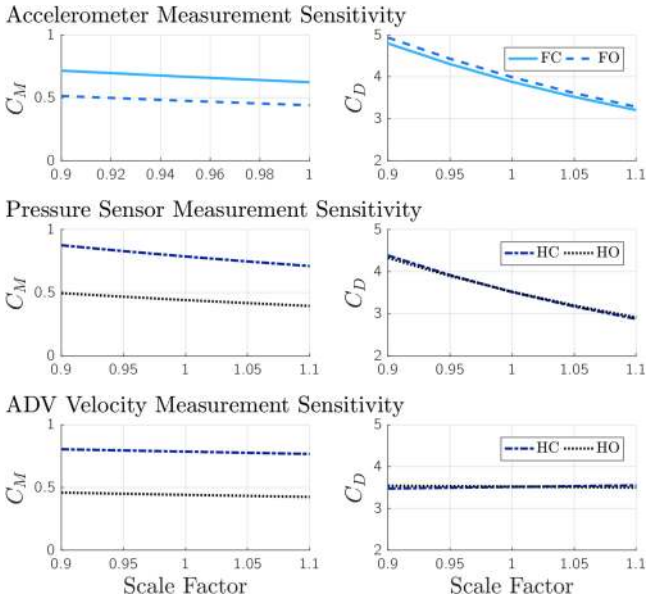

Fig. 13. Sensitivity analysis was conducted to determine the effect of motion sensor error on C_M and C_D. The amplitude of each sensor signal was varied independently, and the effects on the calculated constant coefficients were determined. The sensitivity analysis for IMU acceleration was done using the flat plate data, and the analyses for the pressure and velocity measurements were completed using the data from the hexagonal conic heave plate tests. FC = closed flat plate; FO = open flat plate; HC = closed hexagonal conic; and HO = open hexagonal conic.

and quantity of instantaneous coefficient data increases for vary oscillation amplitudes and frequencies, it may become possible to improve the accuracy of WEC numerical models with intracycle specification of hydrodynamics coefficients.

Appendix
Experimental Error and Coefficient Sensitivity

The friction between the Oscillator thrust rod and guide bearing was investigated in a separate set of experiments from those discussed Section II-A. Tests were run without a heave plate over a range of oscillation amplitudes and frequencies spanning the range discussed in this paper. The force recorded in these tests was primarily due to the inertia of the rod. Dynamic buoyancy, added mass, form drag, and viscous drag were also separated from the recorded force using the same procedure discussed in Section II-C. The remaining residual force is attributed to friction between the guide bearing and shaft. Over all tests run without a heave plate, the frictional force is approximately normally distributed with an RMS value of less than 3 N (see Fig. 12).

The frictional force depends primarily on the normal force of the rod against the wall of the bearing. As the bearing serves only to guide the motion of the thrust rod, the normal force of the shaft on the bearing wall is highly variable. However, the frictional force does tend to peak during periods of peak acceleration for this reason, the RMS values of the frictional force for each test, run without a heave plate, are shown in Fig. 12 plotted against the RMS acceleration of the oscillation.

The failure of the accelerometer during the miniWEC tests of the hexagonal conic heave plate made it necessary to estimate the motion of the heave plates using the measurements provided by the Nortek Signature ADV, which was also mounted to the heave plates. The two measurements are hydrostatic pressure and water velocity. The motion of the heave plate affects both of these measurements, and they are therefore less accurate than the estimate of motion derived from the IMU accelerometer. The fusion of these measurements is discussed in Section II-B. The following analysis quantifies the change in the estimate of C_M and C_D due to measurement error from each sensor.

The hydrodynamic coefficients were recalculated after scaling the amplitudes of each sensor independently. The sensors were scaled over a range of $\pm 10\%$ of the original signal. The results of the analyses are shown in Fig. 13. For the flat plate tests, a 10% change in acceleration amplitude results in a ± 0.08 change to C_M and a ± 0.8 change to C_D. For the hexagonal conic test, the calculated coefficients are most sensitive to error in the pressure measurement with a 10% change resulting a change of ± 0.08 to C_M and ± 0.75 to C_D. The analysis is relatively insensitive to error in the velocity signal due to the low weighting it receives during the fusion of the sensors. However, as both sensors are still weighted by the least squares optimization, the fused estimate of heave plate motion derived from both pressure and velocity is superior to the estimate derived from either sensor individually.

C_M and C_D are also sensitive to error in the synchronization of the various sensors. Iteration was used to find the value of t_{sync} that minimized the error of (6). The values of C_D, C_M, and F_{Mor} were recalculated for each change to t_{sync}. This method of clock synchronization assumes that the Morison equation will most accurately predict the measured force and minimize E_{RMS} when the two clocks are precisely synchronized. Since this requires a strong signal-to-noise ratio, only periods of active wake excitation were used for time synchronization and the calculation of hydrodynamic coefficients. The value of t_{sync} that minimized the residual error of (6) was identified to

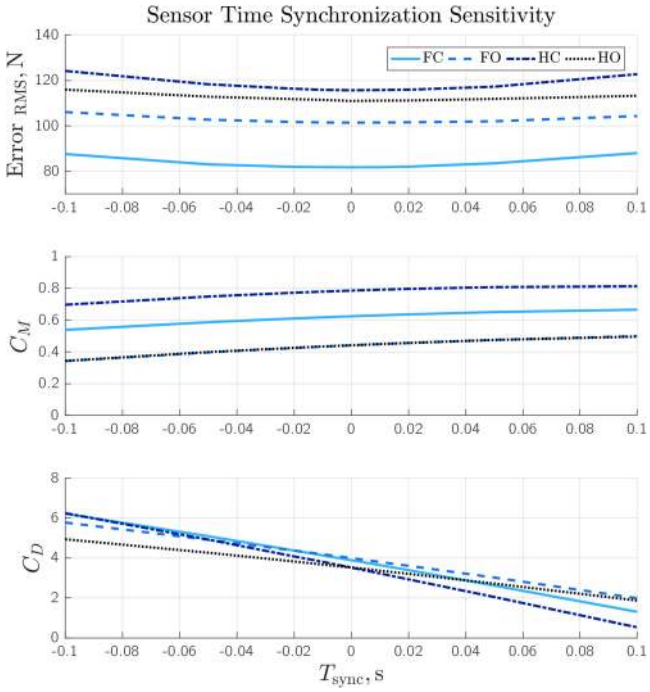

Fig. 14. Effects of sensor time synchronization on the C_M and C_D are shown. The optimum time synchronization was determined, to within ± 0.01 s, by minimizing the RMS error of the Morison fit to the recorded hydrodynamic force. This was done for each heave plate configuration: FC = closed flat plate; FO = open flat plate; HC = closed hexagonal conic; and HO = open hexagonal conic.

an accuracy of ± 0.01 s for each heave plate. The sensitivity of C_M and C_D to the value of t_{sync} is plotted over a range of ± 0.1 s in Fig. 14. The calculation of C_D is most sensitive to error in t_{sync} for the closed hexagonal conic heave plate; an error of ± 0.01 s results in a change of ± 0.3 to C_D.

ACKNOWLEDGMENT

The authors would like to thank A. de Klerk, D. Dubuque, and P. Gibbs for their work on the Oscillator and miniWEC. They would also like to thank J. Talbert, P. Gibbs, R. Carini, and Captain A. Reay-Ellers for their help in deploying the miniWEC.

REFERENCES

[1] J. Falnes, "A review of wave-energy extraction," *Marine Struct.*, vol. 20, no. 4, pp. 185–201, Oct. 2007.

[2] K. Ruehl, C. Michelen, S. Kanner, M. Lawson, and Y.-H. Yu, "Preliminary verification and validation of WEC-sim, an open-source wave energy converter design tool," in *Proc. ASME 33rd Int. Conf. Ocean, Offshore Arctic Eng.*, 2014, pp. 1–7.

[3] A. F. Davis, J. Thomson, T. R. Mundon, and B. C. Fabien, "Modeling and analysis of a multi degree of freedom point absorber wave energy converter," in *Proc. ASME 33rd Int. Conf. Ocean, Offshore Arctic Eng.*, 2014, Paper V08AT06A046.

[4] J. Ebner, "Dynamics of a tension force-driven wave energy converter," M.S. thesis, Dept. Mech. Eng., University of New Hampshire, Durham, NH, USA, 2014.

[5] S. J. Beatty, "Self-reacting point absorber wave energy converters," Ph.D. dissertation, Dept. Mech. Eng., Univ. Victoria, Victoria, BC, Canada, Jul. 2015.

[6] M. Lake, H. He, A. W. Troesch, M. Perlin, and K. P. Thiagarajan, "Hydrodynamic coefficient estimation for TLP and spar structures," *J. Offshore Mech. Arctic Eng.*, vol. 122, no. 2, pp. 118–124, May 2000.

[7] J. Li, S. Liu, M. Zhao, and B. Teng, "Experimental investigation of the hydrodynamic characteristics of heave plates using forced oscillation," *Ocean Eng.*, vol. 66, pp. 82–91, Jul. 2013.

[8] J. R. Morison, J. W. Johnson, S. A. Schaaf, and others, "The force exerted by surface waves on piles," *J. Petroleum Technol.*, vol. 2, no. 5, pp. 149–154, 1950.

[9] G. H. Keulegan and L. H. Carpenter, "Forces on cylinders and plates in an oscillating fluid," *J. Res. Nat. Bureau Standards*, vol. 60, no. 5, May 1958, pp. 423–440.

[10] F. White, *Fluid Mechanics*, 8th ed. New York, NY, USA: McGraw-Hill, Jan. 2015.

[11] G. G. Stokes, "On the effect of the internal friction of fluids on the motion of pendulums," *Trans. Cambridge Philosoph. Soc.*, vol. 9, p. 8, 1851, pp. 1–86.

[12] H. Lamb, *Hydrodynamics*, 6th ed. New York, NY, USA: Dover, 1945.

[13] J. N. Newman, *Marine Hydrodynamics*. Cambridge, MA, USA: MIT Press, Jan. 1977.

[14] C. A. Garrido-Mendoza, K. P. Thiagarajan, A. Souto-Iglesias, B. Bouscasse, and A. Colagrossi, "Numerical investigation of the flow features around heave plates oscillating close to a free surface or seabed," in *Proc. ASME 33rd Int. Conf. Ocean, Offshore Arctic Eng.*, 2014, Paper V007T12A014.

[15] L. Tao and D. Dray, "Hydrodynamic performance of solid and porous heave plates," *Ocean Eng.*, vol. 35, no. 10, pp. 1006–1014, Jul. 2008.

[16] R. G. Dean and R. A. Dalrymple, *Water Wave Mechanics for Engineers and Scientists*. Singapore: World Scientific, 1991.

[17] A. Roshko, "On the development of turbulent wakes from vortex streets," California Institute of Technology, Pasadena, CA, USA, Tech. Rep. 1191, 1954.

[18] A. B. Basset, "On the motion of a sphere in a viscous liquid," *Philosoph. Trans. Roy. Soc. Lond. A*, vol. 179, pp. 43–63, 1888.

[19] L. Cavaleri and E. Mollo-Christensen, "Wave response of a spar buoy with and without a damping plate," *Ocean Eng.*, vol. 8, no. 1, pp. 17–24, Jan. 1981.

[20] J. Wang, S. Berg, Y. H. Luo, A. Sablok, and L. Finn, "Structural design of the truss spar: An overview," in *Proc. 11th Int. Offshore Polar Eng. Conf.*, Jan. 2001, pp. 1–8.

[21] O. M. Faltinsen, *Hydrodynamics of High-Speed Marine Vehicles*. Cambridge, MA, USA: Cambridge Univ. Press, 2006. [Online]. Available: http://ebooks.cambridge.org/ref/id/CBO9780511546068

[22] L. Tao, B. Molin, Y. M. Scolan, and K. Thiagarajan, "Spacing effects on hydrodynamics of heave plates on offshore structures," *J. Fluids Struct.*, vol. 23, no. 8, pp. 1119–1136, Nov. 2007.

[23] L. Tao and K. Thiagarajan, "Low KC flow regimes of oscillating sharp edges. I. Vortex shedding observation," *Appl. Ocean Res.*, vol. 25, no. 1, pp. 21–35, Feb. 2003.

[24] S. An and O. M. Faltinsen, "An experimental and numerical study of heave added mass and damping of horizontally submerged and perforated rectangular plates," *J. Fluids Struct.*, vol. 39, pp. 87–101, 2013.

[25] L. Tao and K. Thiagarajan, "Low KC flow regimes of oscillating sharp edges. II. Hydrodynamic forces," *Appl. Ocean Res.*, vol. 25, no. 2, pp. 53–62, Apr. 2003.

[26] M. I. Rosvoll, "Calculation of added mass in the proximity of the seabed for an oscillating disc," Ph.D. dissertation, Dept. Marine Technol., Norwegian Univ. Sci. Technol., Trondheim, Norway, 2012.

[27] W.-J. Shen, Y.-G. Tang, and L.-Q. Liu, "Research on the hydrodynamic characteristics of heave plate structure with different form edges of a spar platform," *China Ocean Eng.*, vol. 26, no. 1, pp. 177–184, Mar. 2012.

[28] M. J. Downie, J. M. R. Graham, C. Hall, A. Incecik, and I. Nygaard, "An experimental investigation of motion control devices for truss spars," *Marine Struct.*, vol. 13, no. 2, pp. 75–90, Mar. 2000.

[29] B. Molin, "On the added mass and damping of periodic arrays of fully or partially porous disks," *J. Fluids Struct.*, vol. 15, no. 2, pp. 275–290, Feb. 2001.

[30] K. H. Vu, B. Chenu, and K. P. Thiagarajan, "Hydrodynamic damping due to porous plates," in *Proc. World Sci. Eng. Acad. Soc.*, Greece, 2008, pp. 1–5.

[31] B. Molin, "Hydrodynamic modeling of perforated structures," *Appl. Ocean Res.*, vol. 33, no. 1, pp. 1–11, Feb. 2011.

[32] S. Sudhakar and S. Nallayarasu, "Hydrodynamic responses of spar hull with single and double heave plates in random waves," *Int. J. Ocean Syst. Eng.*, vol. 4, no. 1, pp. 1–18, 2014.

[33] B. Li, Z. Huang, Y. M. Low, and J. Ou, "Experimental and numerical study of the effects of heave plate on the motion of a new deep draft multi-spar platform," *J. Marine Sci. Technol.*, vol. 18, no. 2, pp. 229–246, Nov. 2012.

[34] T. R. Mundon, "Progress in the hydrodynamic design of heave plates for wave energy converters," in *Proc. Int. Conf. Ocean Eng.*, Edinburgh, U.K., Feb. 2016, pp. 1–15.
[35] T. R. Mundon and B. Nair, "Optimization of a magnetostrictive wave energy converter," in *Grand Renewable Energy Proc.*, Tokyo, Japan, Jul. 2014, pp. 1–6.
[36] A. C. Brown and J. Thomson, "Heave plate dynamics for a point absorbing wave energy converter," in *Proc. 3rd Marine Energy Technol. Symp.*, Washington, DC, USA, Apr. 2015, pp. 1–5.
[37] L. Johanning, P. W. Bearman, and J. M. R. Graham, "Hydrodynamic damping of a large scale surface piercing circular cylinder in planar oscillatory motion," *J. Fluids Struct.*, vol. 15, no. 7, pp. 891–908, Oct. 2001.
[38] K. Budal and J. Falnes, "A resonant point absorber of ocean-wave power," *Nature*, vol. 256, no. 5517, pp. 478–479, Aug. 1975. [Online]. Available: http://www.nature.com/nature/journal/v256/n5517/abs/256478a0.html
[39] J. Hals, J. Falnes, and T. Moan, "Constrained optimal control of a heaving buoy wave-energy converter," *J. Offshore Mech. Arctic Eng.*, vol. 133, no. 1, p. 15, Nov. 2010. [Online]. Available: http://dx.doi.org/10.1115/1.4001431
[40] J. A. Hamilton *et al.*, "Results from numerical simulation and field tests of an oceanographic buoy powered by sea waves," in *Proc. 33rd Int. Conf. Ocean, Offshore Arctic Eng.*, San Francisco, CA, USA, Jun. 2014, Paper V09BT09A02.
[41] J. Sjolte, B. Sörby, G. Tjensvoll, and M. Molinas, "Annual energy and power quality from an all-electric wave energy converter array," in *Proc. 15th Int. Power Electron. Motion Control Conf.*, Novi Sad, Serbia, Sep. 2012, pp. 1–7.
[42] C. Wunsch, *The Ocean Circulation Inverse Problem*. New York, NY, USA: Cambridge Univ. Press, 1996.
[43] S. J. Beatty, M. Hall, B. J. Buckham, P. Wild, and B. Bocking, "Experimental and numerical comparisons of self-reacting point absorber wave energy converters in regular waves," *Ocean Eng.*, vol. 104, pp. 370–386, Aug. 2015.

Adam Brown received the Ph.D. degree in mechanical engineering from Oregon State University, Corvallis, OR, USA, in 2014.

He is currently a Postdoctoral Researcher with the University of Washington Applied Physics Laboratory, Seattle, WA, USA. His research has focused on understanding the operational environment and hydrodynamic behavior of offshore renewable energy systems.

Jim Thomson received the Ph.D. degree in applied ocean physics and engineering from Massachusetts Institute of Technology, Cambridge, MA, USA, joint program with the Woods Hole Oceanographic Institution, Woods Hole, MA, USA, in 2006.

In 2006, he joined the University of Washington's Applied Physics Laboratory, Seattle, WA, USA. He also has a joint appointment in the faculty of Civil and Environmental Engineering. He studies waves and currents in the coastal ocean, with an emphasis on field measurements and physical processes. As a member of the Northwest National Marine Renewable Energy Center, he is developing techniques to characterize marine energy sites and support device testing.

Curtis Rusch is currently working toward the Ph.D. degree in the Department of Mechanical Engineering, University of Washington, Seattle, WA, USA.

As an undergraduate, he worked on field measurements of turbulence and ocean waves at the Applied Physics Lab. His current research, with the Northwest National Marine Renewable Energy Center, focuses on the modeling and field testing of wave energy converters and their components to better understand WEC dynamics.